Journal of Materials Chemistry A

Ammonia borane modified zirconium borohydride octaammoniate with enhanced dehydrogenation properties

Journal:	*Journal of Materials Chemistry A*
Manuscript ID:	TA-ART-10-2014-005328.R1
Article Type:	Paper
Date Submitted by the Author:	19-Nov-2014

Complete List of Authors:	Huang, Jianmei; South China University of Technology, Tan, Yingbin; Fudan University, Gu, Qinfen; Australian Synchrotron Company Ltd, Ouyang, Liuzhang; South China University of technology, School of materials science and engineering Yu, Xuebin; Fudan University,, Department of Materials Science, zhu, min; South China University of Technology,

Ammonia borane modified zirconium borohydride octaammoniate with enhanced dehydrogenation properties

Jianmei Huang[a,d], Yingbin Tan[b], Qinfen Gu[c], Liuzhang Ouyang[a,d*], Xuebin Yu[b*], Min Zhu[a,d]

[a] School of Materials Science and Engineering and Key Laboratory of Advanced Energy Storage Materials of Guangdong Province, South China University of Technology, Guangzhou 510641, PR China

[b] Department of Materials Science, Fudan University, Shanghai 200433, PR China

[c] Australian Synchrotron, 800 Blackburn Rd., Clayton 3168, Australia

[d]China-Australia Joint Laboratory for Energy & Environmental Materials, South China University of Technology, Guangzhou, 510641, PR China

Abstract: A new complex system, $Zr(BH_4)_4 \cdot 8NH_3$-$n NH_3BH_3$ (n = 2, 3, 4, 5), was prepared via ball milling of $Zr(BH_4)_4 \cdot 8NH_3$ and NH_3BH_3 (AB). The combination strategy effectively suppressed ammonia release and reduced the dehydrogenation temperature when compared to the individual compounds. In the optimized composition, $Zr(BH_4)_4 \cdot 8NH_3$-4AB, the hydrogen purity was improved to 96.1 mol.% and 7.0 wt.% of hydrogen was released at 100 °C. These remarkable improvements are attributed to the interaction between AB and the NH_3 group in $Zr(BH_4)_4 \cdot 8NH_3$, which enables a more active interaction of $H^{\delta+} \cdots {}^{-\delta}H$. These advanced dehydrogenation properties suggest that $Zr(BH_4)_4 \cdot 8NH_3$-4AB is a promising candidate for potential hydrogen storage applications.

Keywords: Hydrogen storage; metal-boron-nitrogen based hydride; Complex; NH_3 suppression;

*To whom correspondence should be addressed. E-mail:

meouyang@scut.edu.cn (Liuzhang Ouyang); yuxuebin@fudan.edu.cn (Xuebin Yu).

1. Introduction

Hydrogen, as an effective and clean energy carrier, is conducive to the transition from fossil fuels to clean power sources.[1, 2] To realize hydrogen economy, the development of safe, inexpensive, and efficient hydrogen storage materials with moderate operating temperatures is key for new technologies.[3-11] Boron–nitrogen (B–N)-based hydrides have received great attention as potential candidates for solid-state hydrogen storage materials due to their high gravimetric hydrogen densities and favorable dehydrogenation properties.[12-14] Among them, metal borohydride ammoniates ($M(BH_4)_m \cdot nNH_3$, MBAs), which contain both BH_4 and NH_3 groups and dehydrogenate based on the interaction of the hydridic B–H and protic N–H bonds, release hydrogen at a relatively low temperature with fast dehydrogenation reaction kinetics.[15-25]

Recently, zirconium borohydride octaammoniate, $Zr(BH_4)_4 \cdot 8NH_3$, with the highest coordination number of NH_3 groups among all reported MBAs had been synthesized. Upon heating, this compound is capable of rapidly releasing hydrogen at 130 °C. Hence, $Zr(BH_4)_4 \cdot 8NH_3$ is considered as one of the promising chemical hydrogen storage materials. However, 16.3 mol.% of ammonia is released during the dehydrogenation process of $Zr(BH_4)_4 \cdot 8NH_3$, which reduces the dehydrogenation purity and amount, and is an obstacle for its practical utilization in fuel cells. Thus, seeking effective approaches to suppress the generation of ammonia from $Zr(BH_4)_4 \cdot 8NH_3$ is vital.

Several approaches including additive doping, nanoconfinement effects from templates and combination methods have been employed to suppress the release of ammonia from many other MBAs.[15, 26-33] The combination methods have shown the advantages of significant improvement of dehydrogenation purity and maintenance of the relatively high system hydrogen storage capacity. They can be divided into two groups, (i) introduce additional BH_4 groups to balance the NH_3 group

in MBAs,[32] (ii) introduce other materials to effect the excessive NH_3 groups.[29] For the strategy of consuming the excessive NH_3 groups, AB was demonstrated as a good additive. The addition of AB in the MBAs system, such as $LiBH_4 \cdot NH_3$, $Al(BH_4)_3 \cdot 6NH_3$ and $Mg(BH_4)_2 \cdot 6NH_3$, to form H-enriched B–N based hydride composites, significantly increased the H_2 purity.[29, 30, 34] It suggests that AB may be an effective additive used to improve the dehydrogenation purity of $Zr(BH_4)_4 \cdot 8NH_3$.

In this work, we successfully prepared a new H-enriched B-N-based complex system by combining AB with $Zr(BH_4)_4 \cdot 8NH_3$. The combination strategy significantly inhibited the ammonia release compared to the individual compounds. In addition, the dehydrogenation temperature was reduced. A systematic investigation of the dehydrogenation properties and dehydrogenation mechanism was also discussed.

2. Experimental

2.1 Preparation

The starting materials, ammonia borane (99.9%) and lithium borohydride (>95%) were purchased from Sigma–Aldrich. Anhydrous $ZrCl_4$ (>99.5%) and ammonia were obtained from Alfa Aesar. All the materials were used as-received without further purification with the exception of NH_3, which was purified by soda lime prior to use.

$Zr(BH_4)_4$ was prepared by ball milling a mixture of $LiBH_4$ and $ZrCl_4$. In a typical procedure, a mixture of $LiBH_4$ and $ZrCl_4$ in a molar ratio of 6:1 was mechanically milled for 6 h at 300 rpm under an atmosphere of argon using stainless steel spheres with a ball-to-powder ratio of 30:1 at relative ambient temperature (<20 °C). The solid-state $Zr(BH_4)_4$ crystals were obtained directly in the lid of the vial. $Zr(BH_4)_4 \cdot 8NH_3$ was prepared as a white powdery solid upon exposing the $Zr(BH_4)_4$ crystals

to an atmosphere of anhydrous ammonia in an ice-water bath for at least 8 h. The $Zr(BH_4)_4 \cdot 8NH_3$-*n*AB mixtures with various molar ratios (*n* = 2–5) were mechanically milled for 30 min under an atmosphere of argon using stainless steel spheres with a ball-to-powder ratio of 30:1. The milling process was carried out by alternating 6 min of milling and 6 min of rest to avoid an increase in the temperature of the sample in the vial. All handling was performed in a glovebox equipped with a recirculation and regeneration system, which maintained the oxygen and water concentrations below 1 ppm.

2.2 Gas evolution measurements

Hydrogen release property measurements were performed using mass spectrometry (QMS 403) connected to a thermogravimetric analyzer (TG, STA 449 C) by an insulated capillary tube, at a heating rate of 5 °C min^{-1}. Temperature-programmed desorption (TPD) for volumetric quantitative measurements was performed in order to measure the decomposition behavior of the samples on a semi-automatic Sievert's apparatus, connected to a reactor filled with a sample (~ 0.1 g) under an atmosphere of argon (1 bar) at a heating rate of 5 °C min^{-1}. The amounts of H_2 and NH_3 in the emission gas were quantified using gravimetric and volumetric analysis. First, the mass percentage (Wp) and moles per gram (Mp) of gas released from the sample were calculated from the weights of the samples and volumetric analysis results. Subsequently, the mole proportion of H_2 (C_{H2}) and NH_3 (C_{NH3}) were calculated using equations (1) and (2).

$$C_{H2} + C_{NH3} = 1 \quad (1)$$

$$(C_{H2} * 2.02 + C_{NH3} * 17.03) * Mp = Wp \quad (2)$$

2.3 Characterization

High-resolution X-ray powder diffraction (HRXRD) data were collected for $Zr(BH_4)_4 \cdot 8NH_3$-4AB on

a Powder Diffraction Beamline, Australian Synchrotron equipped with a Mythen detector. For phase identification and structure determination, samples were loaded into predried 0.7 mm glass capillary tubes inside an argon atmosphere glove box and sealed with vacuum grease for X-ray diffraction measurements at a wavelength of 1.0329 Å. The chemical bonding in the samples was identified using Fourier transform infrared spectroscopy (FT-IR, Nicolet Nexus 470) in the range of 500 cm^{-1} to 4000 cm^{-1}. The samples tested were pressed with anhydrous potassium bromide (KBr) powder. During the IR measurements, samples were loaded into a closed tube with CaF_2 windows. Solid-state ^{11}B nuclear magnetic resonance (NMR) spectra were measured on a Bruker Avance Digital 400 MHz spectrometer, using a Doty CP-MAS probe with no probe background. The powder samples were spun at 12 kHz using 4 mm ZrO_2 rotors loaded in purified argon atmosphere glove box.

3. Results and discussion

3.1 Dehydrogenation properties

The thermal decomposition behaviors of the $Zr(BH_4)_4 \cdot 8NH_3$-*n*AB (*n* = 0, 2, 3, 4, 5) composites compared with neat AB were measured using synchronous TG-MS (Fig. 1) and TPD (Fig. 2). $Zr(BH_4)_4 \cdot 8NH_3$ showed a single hydrogen desorption peak at 130 °C, accompanied with the emission of ammonia. Neat AB released hydrogen at 110 °C in a two-step process, accompanied with the generation of volatile by-products (ammonia, diborane, and borazine). The combined system of $Zr(BH_4)_4 \cdot 8NH_3$-*n*AB showed a different dehydrogenation performance with a two-step decomposition process. $Zr(BH_4)_4 \cdot 8NH_3$-2AB exhibited an initial hydrogen release peak centered at 78 °C, which was accompanied with the release of a small amount of NH_3. The second decomposition step occured at 115–150 °C and is mainly attributed to the generation of H_2. No other

detrimental gas impurities such as diborane and borazine were detected during the decomposition process. When compared to the dehydrogenation of the individual compounds, the first-step dehydrogenation temperature and weight loss of the $Zr(BH_4)_4{\cdot}8NH_3$-2AB composite (78 °C, 16.0 wt.%) were lower than those of both neat $Zr(BH_4)_4{\cdot}8NH_3$ (130 °C, 22.8 wt.%) and AB (124 °C, 52.2 wt.%). The quantitative gas desorption for $Zr(BH_4)_4{\cdot}8NH_3$-*n*AB (*n* = 0, 2, 3, 4, 5) and neat AB were determined using TPD measurements (Fig. 2). According to the results of weight loss and gas release (Fig. 1c and Fig. 2), the hydrogen purity of this composite was 92.5 mol.% (Fig. 3). The above results indicate that AB can effectively improve the dehydrogenation properties of $Zr(BH_4)_4{\cdot}8NH_3$. On the other hand, $Zr(BH_4)_4{\cdot}8NH_3$ also influences the dehydrogenation performance of AB by suppressing the formation of diborane and borazine during the dehydrogenation reaction. However, the release of ammonia was still detected. Our previous results have demonstrated that the NH_3 groups in $Mg(BH_4)_2{\cdot}6NH_3$ act as a Lewis base for the dehydrogenation of AB.[30] Hence, more AB was introduced to consume the NH_3 groups in $Zr(BH_4)_4{\cdot}8NH_3$ to further enhance the purity of the hydrogen released. By increasing the molar ratio of AB to 3 and 4, the onset dehydrogenation temperature and weight loss decrease. The hydrogen purity reaches a maximum of 96.1 mol.% for the $Zr(BH_4)_4{\cdot}8NH_3$-4AB composite. The above results indicate that AB may interact with the NH_3 groups in the composite and thus suppresses the evolution of ammonia while accelerating the release of hydrogen from $Zr(BH_4)_4{\cdot}8NH_3$. Upon increasing the molar ratio of AB to 5, the weight loss increased while the gas release was reduced, resulting in a decrease in the hydrogen purity to 92.7 mol.%. This suggests that the excess AB decomposes causing the evolution of ammonia by autolysis. From the above results, it can be concluded that the addition of an appropriate amount of AB is capable of improving the dehydrogenation properties of $Zr(BH_4)_4{\cdot}8NH_3$ by suppressing the evolution

of ammonia and decreasing the dehydrogenation temperature.

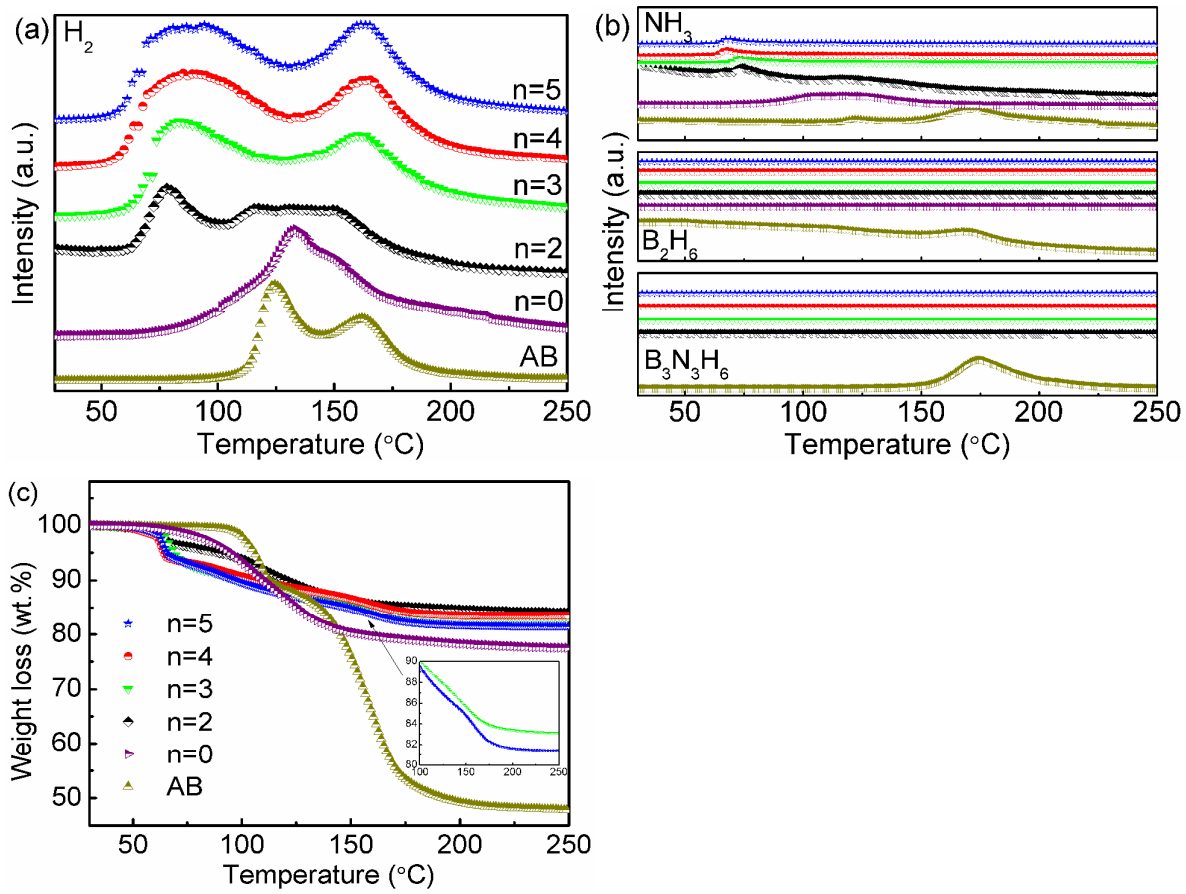

Fig. 1 (a) , (b) MS and (c) TG profiles of $Zr(BH_4)_4 \cdot 8NH_3$-nAB (n = 0, 2, 3, 4, 5) and neat AB with a heating rate of 5 °C min^{-1} in argon.

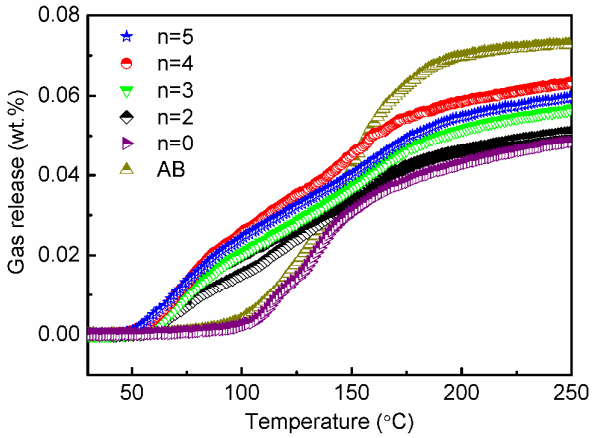

Fig. 2 TPD profiles of $Zr(BH_4)_4 \cdot 8NH_3$-nAB (n = 0, 2, 3, 4, 5) and neat AB with a heating rate of 5 °C min^{-1} in argon.

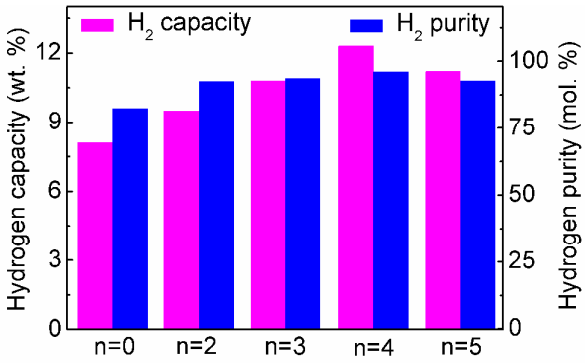

Fig. 3 Summary of hydrogen release capacity and purity.

The enhanced dehydrogenation behavior for the $Zr(BH_4)_4 \cdot 8NH_3$-4AB composite was further demonstrated by measuring the isothermal desorption kinetics from 80 to 130 °C (Fig. 4) and compared with $Zr(BH_4)_4 \cdot 8NH_3$ and AB. Only 0.18 wt.% and 2.0 wt.% of hydrogen were released from AB and $Zr(BH_4)_4 \cdot 8NH_3$ within 60 min at 80 °C and 90 °C, respectively. However, for $Zr(BH_4)_4 \cdot 8NH_3$-4AB, 5.1 wt.% of hydrogen was released within 60 min at 80 °C. Elevating the temperature enhanced the dehydrogenation capacity and accelerated kinetics, i.e., 7.0 wt.%, 9.2 wt.% and 10.7 wt.% of H_2 could be eliminated at 100 °C, 115 °C and 130 °C, respectively. These results reveal that the dehydrogenation kinetics of the $Zr(BH_4)_4 \cdot 8NH_3$-4AB composite were significantly enhanced when compared to AB and $Zr(BH_4)_4 \cdot 8NH_3$. However, as the dehydrogenation of the $Zr(BH_4)_4 \cdot 8NH_3$-4AB composite was exothermic (Fig. S1), it was not able to rehydrogenate directly by charging with hydrogen.

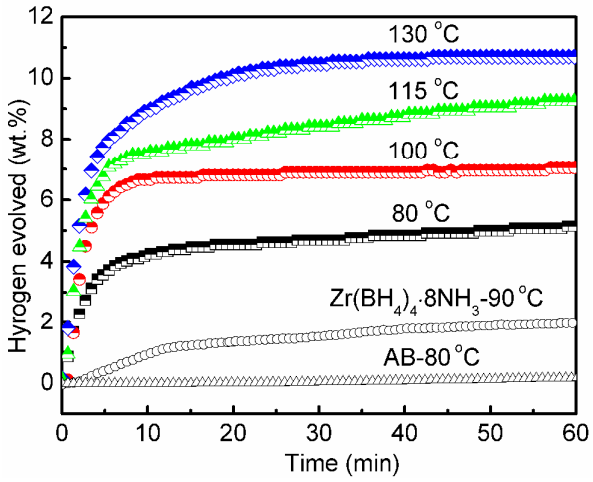

Fig. 4 Isothermal dehydrogenation results for $Zr(BH_4)_4 \cdot 8NH_3$-4AB at 80 °C, 100 °C, 115 °C and 130 °C, compared with AB at 80 °C and $Zr(BH_4)_4 \cdot 8NH_3$ at 90 °C.

3.2 Decomposition process

To clarify the mechanism of ammonia suppression and dehydrogenation enhancement, the decomposition products of $Zr(BH_4)_4 \cdot 8NH_3$-4AB were studied using high-resolution *in-situ* XRD, and FT-TR and ^{11}B NMR spectroscopy. As shown in Fig. 5a, all the diffraction peaks in the $Zr(BH_4)_4 \cdot 8NH_3$-4AB prepared can be indexed as $Zr(BH_4)_4 \cdot 8NH_3$ and AB and no new phases were observed, indicating that the $Zr(BH_4)_4 \cdot 8NH_3$-4AB composite was a result of mechanical physical mixing. From the high-resolution *in-situ* XRD (Fig. 5b), it could be observed that the intensity of all the diffraction peaks of $Zr(BH_4)_4 \cdot 8NH_3$ increased at 50 °C, which was due to an increase in the crystallinity of the sample at elevated temperatures. Sequentially, those diffraction peaks dramatically reduced as the temperature was increased from 50 to 110 °C, and finally disappeared at 120 °C. The intensities of the peaks assigned to AB decreased faster than those of $Zr(BH_4)_4 \cdot 8NH_3$, and vanished at 80 °C. It is notable that the temperature at which the peak vanished for the $Zr(BH_4)_4 \cdot 8NH_3$ phase in the $Zr(BH_4)_4 \cdot 8NH_3$-4AB composite was lower than that in $Zr(BH_4)_4 \cdot 8NH_3$

(130 °C), indicating that the introduction of AB reduces the dehydrogenation temperature of $Zr(BH_4)_4{\cdot}8NH_3$, which was in agreement with the MS results (Fig. 1a).

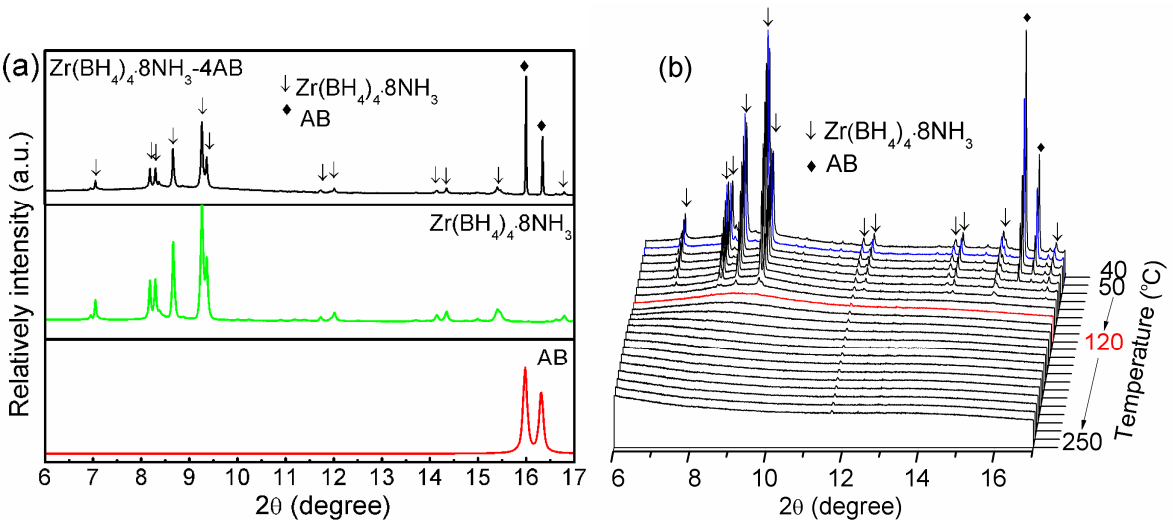

Fig. 5 (a) High-resolution XRD profiles for $Zr(BH_4)_4{\cdot}8NH_3$-4AB and $Zr(BH_4)_4{\cdot}8NH_3$; (b) High-resolution *in situ* XRD profiles for $Zr(BH_4)_4{\cdot}8NH_3$-4AB measured every 10 °C with a heating rate of 3 °C min^{-1} in argon. λ = 1.0329 Å.

The dehydrogenation mechanism for $Zr(BH_4)_4{\cdot}8NH_3$-4AB was further determined using FT-IR spectra collected at various temperatures (Fig. 6a). AB showed characteristic absorption peaks, which were attributed to the stretching N–H bands in the region between 3050 and 3350 cm^{-1}, bending N–H band at 1376 cm^{-1}, stretching B–H bands in the region between 2210 and 2520 cm^{-1}, and two symmetrical bending B–H bands in the region between 1000 and 1200 cm^{-1}. $Zr(BH_4)_4{\cdot}8NH_3$ exhibited stretching and bending B–H bands in the regions between 2180–2470 cm^{-1} and 1000–1280 cm^{-1}, and stretching and bending N–H bands in a broad region ranging from 2950 to 3330 cm^{-1} and 1405 cm^{-1}, respectively. When compared to neat $Zr(BH_4)_4{\cdot}8NH_3$ and AB, the $Zr(BH_4)_4{\cdot}8NH_3$-4AB composite at 25 °C contained all the vibration peaks of $Zr(BH_4)_4{\cdot}8NH_3$ and AB. Upon increasing the

temperature to 70 °C, the B–H vibrations assigned to AB at 780 cm^{-1} and 1000–1200 cm^{-1}, and the N–H vibrations assigned to $Zr(BH_4)_4 \cdot 8NH_3$ decreased simultaneously. However, amlost no change of typical features of the $[BH_4]^-$ group of $Zr(BH_4)_4 \cdot 8NH_3$ in the regions of 2180–2470 cm^{-1}. The results indicate the BH_3 in AB may interact with the NH_3 group in $Zr(BH_4)_4 \cdot 8NH_3$. This observation corresponds with our previous works which have demonstrated that in the presence of NH_3, the dehydrogenation of AB can be promoted due to the fact that the protic N-H bonds of NH_3 are more reactive than those in AB toward the hydride B-H, leading to the fast evolution of hydrogen at a relatively low temperature. [29, 34] Further elevating the temperature to 130 °C, the intensity of the N–H and B–H absorptions were further reduced and then almost vanished after heating to 250 °C, accompanied with the formation of a B–N band ranging from 1250 cm^{-1} to 1550 cm^{-1}. These results suggest that the consumption of N–H and B–H and the formation of a B–N-like residue during the dehydrogenation of $Zr(BH_4)_4 \cdot 8NH_3$-4AB, which is in agreement with the DSC results of exothermic reaction. The formation of the B–N polymer upon dehydrogenation was further confirmed using ^{11}B NMR spectroscopy (Fig. 6b). After dehydrogenation at 250 °C, three boron signals at 4.47, 15.2 and 25.3 ppm appeared, together with two tetracoordinate boron signals at –16.9 and –37 ppm, which corresponded to $BH_3(N)$ and BH_4^- residues, respectively.

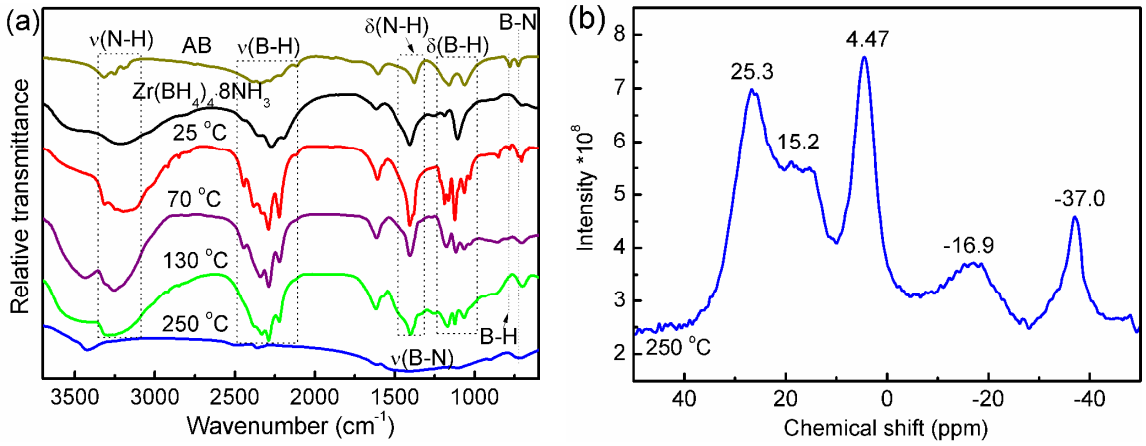

Fig. 6 (a) FT-IR spectra for $Zr(BH_4)_4 \cdot 8NH_3$-4AB at 25 °C, 70 °C, 130 °C and 250 °C, compared with the neat AB and $Zr(BH_4)_4 \cdot 8NH_3$; (b) ^{11}B NMR spectra for $Zr(BH_4)_4 \cdot 8NH_3$-4AB at 250 °C.

Based on the above results, the dehydrogenation of $Zr(BH_4)_4 \cdot 8NH_3$-4AB occurs through a combination of the BH and NH groups, resulting in the formation of an amorphous B-N based polymer. The improved dehydrogenation performance is a result of the interaction between AB and the NH_3 groups in $Zr(BH_4)_4 \cdot 8NH_3$, resulting in a decrease in the coordination number of NH_3 on the Zr cations. Hence, the dehydrogenation purity and temperature of $Zr(BH_4)_4 \cdot 8NH_3$ were improved by the combination of AB.

4. Conclusions

A new hydrogen storage system, $Zr(BH_4)_4 \cdot 8NH_3$-*n*AB (*n* = 2, 3, 4, 5) was prepared *via* simple ball milling of $Zr(BH_4)_4 \cdot 8NH_3$ and AB. When compared to $Zr(BH_4)_4 \cdot 8NH_3$ and pure AB, these composites show a mutual dehydrogenation improvement in terms of suppressed toxic by-product gas formation, decreased hydrogen evolution temperature, and enhanced dehydrogenation kinetics. The optimized composition, $Zr(BH_4)_4 \cdot 8NH_3$-4AB, exhibits the first dehydrogenation peak centered at 85 °C, a maximum hydrogen purity of 96.1 mol.% and the release of 7.0 wt.% of hydrogen within 45 min at 100 °C. This significant improvement is attributed to the interaction of AB and the NH_3 groups in $Zr(BH_4)_4 \cdot 8NH_3$, which leads to a decrease in the coordination number of NH_3 on the Zr cations. This study demonstrates a novel potential candidate hydrogen storage material and further confirms the effective strategy of synthesis and modification of metal-boron-nitrogen based hydrides with modulated hydrogen storage performance.

Acknowledgements

This work was supported by the National Natural Science Foundation of China Projects (Nos. 51431001, 51271078, U120124 and 21271046), by GDUPS (2014) and by KLGHEI (KLB11003). Part of this research was undertaken on the Powder Diffraction beamline at the Australian Synchrotron, Victoria, Australia.

References

1. L. Schlapbach and A. Zuttel, *Nature*, 2001, **414**, 353-358.
2. K. Mazloomi and C. Gomes, *Renew. Sust. Energy Rev.*, 2012, **16**, 3024-3033.
3. L. Z. Ouyang, Y. J. Xu, H. W. Dong, L. X. Sun and M. Zhu, *Int. J. Hydrogen Energy*, 2009, **34**, 9671-9676.
4. A. Züttel, *Mater. Today*, 2003, **6**, 24-33.
5. P. Chen and M. Zhu, *Mater. Today*, 2008, **11**, 36-43.
6. J. Huang, Y. Yan, L. Ouyang, H. Wang, J. Liu and M. Zhu, *Dalton T.*, 2014, **43**, 410-413.
7. S.-i. Orimo, Y. Nakamori, J. R. Eliseo, A. Züttel and C. M. Jensen, *Chem. Rev.*, 2007, **107**, 4111-4132.
8. T. K. Nielsen, F. Besenbacher and T. R. Jensen, *Nanoscale*, 2011, **3**, 2086-2098.
9. L. Ouyang, S. Ye, H. Dong and M. Zhu, *Appl. Phys. Lett.*, 2007, **90**, 021917-021917-021913.
10. L. Ouyang, H. Wang, C. Chung, J. Ahn and M. Zhu, *J. Alloy Compd.*, 2006, **422**, 58-61.
11. L. Z. Ouyang, Y. J. Wen, Y. J. Xu, X. S. Yang, L. X. Sun and M. Zhu, *Int. J. Hydrogen Energy*, 2010, **35**, 8161-8165.

12. G. Kresse and J. Furthmuller, *Phys. Rev. B.*, 1996, **54**, 11169-11186.

13. A. Staubitz, A. P. Robertson and I. Manners, *Chem. Rev.*, 2010, **110**, 4079-4124.

14. Y. S. Chua, P. Chen, G. Wu and Z. Xiong, *Chem. Commun.*, 2011, **47**, 5116-5129.

15. Y. Guo, G. Xia, Y. Zhu, L. Gao and X. Yu, *Chem. Commun.*, 2010, **46**, 2599-2601.

16. G. Soloveichik, J.-H. Her, P. W. Stephens, Y. Gao, J. Rijssenbeek, M. Andrus and J. C. Zhao, *Inorg. Chem.*, 2008, **47**, 4290-4298.

17. H. Chu, G. Wu, Z. Xiong, J. Guo, T. He and P. Chen, *Chem. Mater.*, 2010, **22**, 6021-6028.

18. Y. Guo, X. Yu, W. Sun, D. Sun and W. Yang, *Angew.Chem. Int. Ed.*, 2011, **50**, 1087-1091.

19. F. Yuan, Q. Gu, Y. Guo, W. Sun, X. Chen and X. Yu, *J. Mater. Chem.*, 2012, **22**, 1061-1068.

20. Z. Tang, F. Yuan, Q. Gu, Y. Tan, X. Chen, C. M. Jensen and X. Yu, *Acta. Mater.*, 2013, **61**, 3110-3119.

21. G. Xia, Q. Gu, Y. Guo and X. Yu, *J. Mater. Chem.*, 2012, **22**, 7300-7307.

22. Q. F. Gu, L. Gao, Y. H. Guo, Y. B. Tan, Z. W. Tang, K. S. Wallwork, F. W. Zhang and X. B. Yu, *Energy Environ. Sci.*, 2012, **5**, 7590-7600.

23. Y. Yang, Y. Liu, H. Wu, W. Zhou, M. Gao and H. Pan, *Phys. Chem. Chem. Phys.*, 2014, **16**, 135-143.

24. K. Wang, J.-G. Zhang, J.-S. Jiao, T. Zhang and Z.-N. Zhou, *J. Phys. Chem. C*, 2014, **118**, 8271-8279.

25. Y. Yang, Y. Liu, Y. Li, M. Gao and H. Pan, *J. Phys.Chem. C*, 2013, **117**, 16326-16335.

26. Z. Tang, Y. Tan, H. Wu, Q. Gu, W. Zhou, C. M. Jensen and X. Yu, *Acta Mater.*, 2013, **61**, 4787-4796.

27. Z. Tang, Y. Tan, X. Chen, L. Ouyang, M. Zhu, D. Sun and X. Yu, *Angew. Chem. Int. Ed.*,

2013, **125**, 12891-12895.

28. S. Li, W. Sun, Z. Tang, Y. Guo and X. Yu, *Int. J. Hydrogen Energy*, 2012, **37**, 3328-3337.

29. Y. Tan, Q. Gu, J. A. Kimpton, Q. Li, X. Chen, L. Ouyang, M. Zhu, D. Sun and X. Yu, *J. Mater. Chem. A*, 2013, **1**, 10155-10165.

30. X. Chen, F. Yuan, Q. Gu, Y. Tan, H. Liu, S. Dou and X. Yu, *Int. J. Hydrogen Energy*, 2013, **38**, 16199-16207.

31. Y. Guo, Y. Jiang, G. Xia and X. Yu, *Chem. Commun.*, 2012, **48**, 4408.

32. Y. Guo, H. Wu, W. Zhou and X. Yu, *J. Am. Chem. Soc.*, 2011, **133**, 4690-4693.

33. W. W. Sun, X. W. Chen, Q. F. Gu, K. S. Wallwork, Y. B. Tan, Z. W. Tang and X. B. Yu, *Chem. Eur. J.*, 2012, **18**, 6825-6834.

34. Y. Tan, Y. Guo, S. Li, W. Sun, Y. Zhu, Q. Li and X. Yu, *J. Mater. Chem.*, 2011, **21**, 14509-14515.

Table of Contents Entry

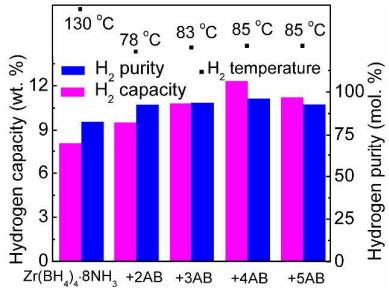

The dehydrogenation purity and temperature of $Zr(BH_4)_4 \cdot 8NH_3$ were improved by combination of NH_3BH_3 (AB).